

RSC Advances



This is an *Accepted Manuscript*, which has been through the Royal Society of Chemistry peer review process and has been accepted for publication.

Accepted Manuscripts are published online shortly after acceptance, before technical editing, formatting and proof reading. Using this free service, authors can make their results available to the community, in citable form, before we publish the edited article. This *Accepted Manuscript* will be replaced by the edited, formatted and paginated article as soon as this is available.

You can find more information about *Accepted Manuscripts* in the [Information for Authors](#).

Please note that technical editing may introduce minor changes to the text and/or graphics, which may alter content. The journal's standard [Terms & Conditions](#) and the [Ethical guidelines](#) still apply. In no event shall the Royal Society of Chemistry be held responsible for any errors or omissions in this *Accepted Manuscript* or any consequences arising from the use of any information it contains.

Polyhedral Oligomeric Silsesquioxane Compositing Gel Polymer Electrolyte Based on Matrix of PMMA

Yun Huang^{a,*}, Sheng-Dong Gong^a, Rui Huang^a, Hai-Jun Cao^{b,*}, Yuan-Hua Lin^a, Man
Yang^a, Xing Li^a

^a School of Materials Science and Engineering, Southwest Petroleum University, Chengdu, 610500, China.

^b Institute of Blood Transfusion, Chinese Academy of Medical Sciences, Chengdu, 610052, China.

* Corresponding author. Tel.: +86 028 83037409.
E-mail address: huangyun982@163.com (Y. Huang).
chj007@163.com (H.J. Cao).

Abstract: The present research is based on the both expectations: polyhedral oligomeric silsesquioxane (POSS) nano-cage can endow gel polymer electrolyte (GPE) with similar modification caused by other inorganic nano-particles; the organic substituents on the cage corners make POSS be more compatible with GPE. So POSS as hybrid modification filler was added into the GPE with polymethyl methacrylate (PMMA) matrix. The results indicated that POSS addition amount was a critical factor for the ionic conductivity of prepared GPEs. When POSS content was 7.5wt.%, the thermal stability was sufficient at the elevated temperature; the ionic conductivity of GPE reached up to $2.0 \times 10^{-3} \text{ S cm}^{-1}$; the mechanism of conductivity was the typical Arrhenius behavior; the lithium ion transference number was up to 0.33; the deposition/dissolution of lithium was highly reversible; the electrochemical stability window was high enough with 5.25V and the compatibility of electrolyte with lithium electrolyte was satisfying.

Keywords: Gel polymer electrolyte; Polymethyl methacrylate; Vinyl trimethoxy silane; Polyhedral oligomeric silsesquioxane

1. Introduction

Lithium ion batteries (LIBs) have been attracted much attention in the last decade for their wide application in digital products and vehicles, etc.¹⁻⁶ Now, the electrolyte commonly used in LIBs is liquid electrolyte which has its own advantages such as low cost, high ionic conductivity and better compatibility with electrode.⁷ But it also has some shortcomings such as liquid leakage, flame and explosion,⁸ which compels many researchers devote to develop some novel electrolytes to improve application performances in batteries.⁹⁻¹⁵ Gel polymer electrolyte (GPE) is one kind of potential electrolyte and is provided with high ionic conductivity, better compatibility with electrode, free shape flexibility and safety etc.¹⁶⁻²³ GPE is considered as the optimal electrolyte and even the key point to further improve properties of LIBs. But GPE still has existed one fatal problem: the increased mechanical property and better membrane self-standing usually are based on the sacrifice of ionic conductivity. So many researches have been carried out to improve comprehensive properties of GPE and to quest for achieving these following basic requirements at the same time:²⁴⁻²⁷ (i) ionic conductivity higher than 10^{-4} Scm^{-1} at room temperature, (ii) good

thermal stability, (iii) considerable electrochemical properties, (iv) high enough mechanical strength, (v) self-standing. Many effective methods and research directions have been adopted to accomplish the target. The most outstanding artifice is the incorporation of inorganic nano-particles filler into GPE.²⁸⁻³⁵ The obtained research results reveal that inorganic nano-particles filler usually improves GPE performances through the following micro-effects: the capillary action produced by nano-particles can tightly capture the plasticizer in GPE and obviously increase ionic conductivity and electrochemical stability of GPE;³⁶ the Lewis acid and base action exists between nano-particles and lithium salt in GPE can promote the dissociation extent of lithium salt and enhance the conductivity;³⁷ the tremendous surface of nano-particles endows GPE with improved mechanical strength and easy membrane formation.³⁸ However, the high surface energy from large surface area of all inorganic nano-particles usually leads to particle agglomeration, which negates any benefits from nano-particles.³⁹ In order to overcome the aforementioned distinct drawback and at the same time retain all advantages of nano-particles, here a facile and efficient route is to incorporate organic-inorganic hybrid particle of polyhedral oligomeric silsesquioxane (POSS) into GPE.

POSS particle is a class of discrete, 3-dimensional polycyclic compound and has received widespread interest due to their cage-like molecular structure, and its empirical formula follows the $(\text{RSiO}_{1.5})_n$, where 'n' is an integer and can be 8, 10 or 12 and R can be a range of organic substituents.⁴⁰ The POSS nano-cage is surrounded by eight organic groups, and is highly soluble in organic/inorganic materials.⁴¹⁻⁴² The POSS nano-cage can endow GPE with similar modification inorganic nano-particles have done. Meanwhile the organic substituents on the cage corners make POSS be hydrophobic and so compared with other inorganic nano-particles, POSS is more compatible with GPE.

Until now the related publications about POSS modified GPE have not been reported. The present work firstly introduced the POSS composited GPE based on the matrix of polymethyl methacrylate (PMMA) in the field of electrolytes used in LIBs. Here there are objectives: POSS particle was synthesized from vinyl trimethoxy silane (VTMS) and then further was characterized; PMMA, plasticizer of propylene carbonate (PC), lithium perchlorate (LiClO_4) and POSS were chosen to prepare POSS modified GPEs, and subsequently the comprehensive performances of GPEs were investigated. In this research, we reported a preliminary study demonstrating the

feasibility of POSS modified GPE.

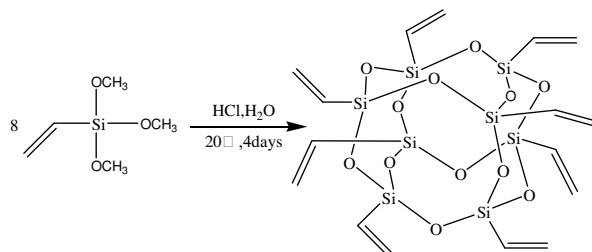
2. Experimental

2.1. Materials

Polymethyl methacrylate (PMMA) with average molecular weight in the level of 10^5 g mol^{-1} , ethyl acetate(EA,AR), hydrochloric acid(AR), anhydrous lithium perchlorate (LiClO_4 , AR), propylene carbonate(PC, AR) were obtained from Chengdu Kelong Company. Vinyl trimethoxy silane (VTMS, CP) was obtained from Nanjing UP Chemical.

2.2. Synthesis of POSS

200ml EA and 20ml VTMS were mixed in 3 neck glass reactor equipped with a reflux condenser, an additional funnel and a mechanical stirrer under stirring at room temperature for 10 min. The mixed solution of 30ml HCl and 70ml deionized water was added in the additional funnel, and was then dropped into the glass reactor within 30min. The reaction was carried out under stirring vigorously for 4 days. The reaction solution was filtrated and then the white solid product recrystallized with acetone was produced. **Scheme.1** presents the synthesis reaction.



Scheme.1 The synthesis reaction of POSS.

2.3. Preparation of GPE films

The PMMA of 1.000, 0.990, 0.975, 0.950, 0.925 or 0.900g was dissolved in acetone at 70°C in one seal glass cup for about 1 hour, and then a certain corresponding amount of 0.000, 0.010, 0.025, 0.050, 0.075 or 0.100 POSS was dispersed in the resulting mixture for 2 hours under the same temperature. The resulted solution was casted on a PTFE plate to allow acetone to evaporate slowly at room temperature. Two days later, this procedure yielded mechanic stable and free standing transparent dry film with uniform thickness. Liquid electrolyte was previously prepared by dissolving LiClO_4 in plasticizer PC to obtain the solution with concentration of 1 mol L^{-1} . The dry film was then immersed into liquid electrolyte to soak the plasticizer. The final plasticizer

saturated film was the expected GPE. Table.1 listed the prepared GPEs with different POSS addition amount.

The liquid electrolyte uptake (A) of membrane is determined by immersing it in liquid electrolyte for enough time, and is calculated by equation (1):

$$A = \frac{W_2 - W_1}{W_1} \times 100\% \quad (1)$$

Where W_1 is the mass of dry membrane and W_2 is the mass of the wet membrane.

2.4. Characterization

The composition and structure of POSS were characterized by Fourier transform infrared spectroscopy (FTIR) (Perkin Elmer Spectrum 2000 series spectrometer) in the range of 4000~400 cm^{-1} with a nominal resolution of 2 cm^{-1} . Spectrum 2000 spectrometer is equipped with a DGTS detector and a Perkin Elmer MIR-IR source, using a conventional short-pathway IR gas cell Wilmad (New Jersey, USA) with 10 cm of pathway and 60 ml internal volume, equipped with 32mm \times 2mm circular SeZn windows. The sample of POSS mixed with potassium bromide (KBr) according to the ratio of 1:100 for FTIR analysis was firstly grounded into fine particles using agate mortar and pestle. The mixture sample was transferred into micro-quartz tube for extensive dry. Then sample powder was compressed into a thin disk using pelletizer under 100 kg cm^{-2} pressures for 2min.

The differential scanning calorimetry (DSC) was conducted on METTLER TOLEDO Star DSC 822° model equipped with automatic sampler of TSO801RO in sealed Al pans (40mL) with dry air flow rate of 20mL min^{-1} to survey thermal property of POSS or GPEs in air atmosphere at a heating rate of 10°C min^{-1} ; the error of temperature measurement was 0.2 K. Thermogravimetric analysis (TGA) was conducted on METTLER TOLEDO TGA/SDTA851°/LF/1100°C equipped with automatic sampler of TSO801RO and METTLER TOLEDO Scale of MT5 with the heating rate of 10°C min^{-1} under air atmosphere.

X-ray diffraction (XRD) patterns were obtained by Rigaku miniflex diffractometer ($\text{CuK}\alpha$ as radiation, $\lambda = 0.154 \text{ nm}$) at a generator voltage of 40 kV and a current of 40 mA at room temperature.

The ionic conductivity of GPE was characterized by electrochemical impedance spectra (EIS)

measurement (CHI-660D electrochemical work station, Shanghai CH Instruments Co., China) in an ordinary cell composed of a Teflon tube and two identical stainless steel electrodes (diameter=1cm). The frequency range of the signal was from 0.1 Hz to 100 KHz, and the amplitude of the alternative signal was 10 mV. The GPE was sandwiched between two stainless steel (SS) rectangle (length of a side = 1 cm). The ionic conductivity measurement of GPE is carried out from the complex EIS curve and can be obtained from Equation (2).

$$\sigma = \frac{L}{R_b S} \quad (2)$$

Where L (cm) is the thickness of GPE, R_b (Ω) is the electrolyte bulk resistance and S (cm^2) is the contact area between GPE and SS square.

The lithium-ion transference number was measured using a symmetric cell of Li/GPE/Li by the DC polarization method combined with EIS method. It can be obtained according to the following equation:⁴³

$$t_{\text{Li}^+} = \frac{I_s (\Delta V - R_0 I_0)}{I_0 (\Delta V - R_s I_s)} \quad (3)$$

Where I_0 and I_s are the initial and steady current, respectively; R_0 and R_s are the initial interfacial and steady-state resistance, respectively; ΔV is the DC voltage applied.

The electrochemical stability test (cyclic voltammetry) was conducted in cell Li/GPE/SS using the CHI-660D instrument in the voltage range of -1.0~5.0 V at a scan rate of 5.0 mVs^{-1} . The oxidative stability of GPE was determined on the electrochemical instrument (CHI-660D) by linear sweep voltammetry (LSV) using the cell Li/GPE/SS, in which the SS was used as working electrode, the lithium as the reference and the counter electrodes. The scanning rate is 5.0 mVs^{-1} over the range of 3.0-6.0 V at room temperature.

Time dependant interfacial resistance (R_i) between lithium electrode and GPE was evaluated by monitoring the complex impedance response on Li/PCE/Li cell over a period of 28 days at room temperature. The test was conducted on CHI-660D in the frequency range from 0.1 Hz to 100 KHz and with the amplitude of 10.0 mV.

3. Results and discussion

3.1. POSS characterization

3.1.1. FTIR spectrum analysis

Fig.1 presents the POSS FTIR spectrum. From **Fig.1** the characteristic peaks of POSS are at 1621cm^{-1} for the C=C bond and at 1115cm^{-1} for the symmetric stretching vibrations of the siloxane (Si-O-Si) group which is the characteristic absorption peak of silsesquioxane cages,⁴⁴⁻⁴⁵ respectively. The peak at 778cm^{-1} is the stretching vibrations of Si-C-H group,⁴⁶ and the absorption peaks of Si-CH=CH₂ bending vibration are at 1411cm^{-1} , 973cm^{-1} , 1279cm^{-1} and 1007cm^{-1} , respectively. Therefore, it can be concluded that POSS is successfully synthesized.

3.1.2. XRD analysis

From **Fig.2**, it can be observed that the POSS is a highly crystalline material and has a characteristic dominant diffraction peaks at 19.1° , 20.9° , 22.5° , 23.3° , 27.9° , 29.2° and 30.5° .

3.1.3. Thermal analysis

The thermal stability of POSS is examined by TGA in **Fig.3(a)**. The thermal degradation curve displays decomposition trend starting at 250°C . The decomposition behavior between 250°C and 500°C shows a two-step mass loss process: the first stage of degradation from 250°C to 320°C with the sharp mass loss should be assigned to the decomposition of the alkyl side chains on the corners in POSS cage; the second stage from 320°C to 500°C with the a little slow mass loss should be ascribed to the disintegration of POSS cage. In addition, it can be observed that during the thermal degradation, the residual mass percent always keeps comparatively high, and even the temperature beyond 500°C the residual mass percent is still high (68.8wt.%). This can be attributed to three reasons: firstly, POSS contains a large number of high energy bonds such as Si-O bond and Si-C bond which endows POSS with excellent thermal stability; secondly the cage inorganic structure of POSS is relatively stable and difficult to be collapsed; thirdly, in POSS the inorganic component content of Si which becomes SiO₂ solid in TGA test is massive.

Fig. 3(b) shows the DSC profile for the synthesized POSS. There are three characteristic peaks. The endothermic peak at lower temperature of 121°C is the reflection of organic phase chain

movement. So 121 °C should be the glass transition temperature (T_g) of organic phase formed by the large number of alkyl on the corners of POSS cage structure. At 213 °C, a little broad endothermic peak is the indication of crystalline melting process, so 213 °C should be the melting temperature (T_m) of POSS. The very strong exothermic peak at 300 °C corresponds to the degradation of POSS, which has been proved in above TGA.

3.2. GPE performances

3.2.1. Thermal stability of GPE

The thermal stability of GPE is examined by TGA presented in **Fig.4 (a)**. For all of GPEs, the trends of thermal decomposition are similar. Considered the application temperature of lithium ion batteries, the high temperature of 100 °C is comparatively enough. From the partial enlarged drawing, when the temperature reaches up to 100 °C, the mass loss resulted from the volatilization of plasticizer (PC) in GPE is very small (less than 5wt.%). So it can be concluded that the all prepared GPEs are thermal stable. But there is one very obvious influence of POSS addition amount on the thermal stability. In all GPEs, the mass loss of GPE-0 is the lowest. This can be explained as that because of the capillary action produced by POSS the composited GPEs can adsorb more amount of liquid electrolyte,³⁶ which will be proved in the discussion of ionic conductivity. When temperature increases, of course these composited GPEs release more plasticizer of PC. For five modified GPEs, there is an optimum addition amount of POSS, and GPE-5 and GPE-7.5 appear better thermal stability. In addition, all GPEs appear massive and quick mass loss at the temperature of 225 °C and around 300 °C, respectively. So the GPEs composited by POSS have sufficient thermal stability even at the elevated temperature.

DSC is used to measure GPE for further application in the lithium ion batteries. The DSC curves of GPE are shown in **Fig.4 (b)**. Before 100 °C, the vertical fluctuate range of DSC curves is very weak which is an evidence of none of any obvious endothermic peak. Here it is further approved that five kinds of GPE system composited by POSS are stable in the temperature range from 30 °C to 100 °C and satisfy the higher temperature requirement in actual production application.

The TGA and DSC analysis demonstrate that obtained membranes can withstand temperatures

of up to 100°C without undergoing thermal decomposition and meet the requirements of practical application for flexible lithium ion batteries.

3.2.2. Ionic conductivity

EIS was carried out on cell SS/GPE/SS to determine ionic conductivity. **Fig.5** presents the Nyquist plots of electrochemical impedance at room temperature and reflects the experimentally obtained ionic conductivities of GPEs as a function of POSS addition content. It can be seen from **Table.2** that the ionic conductivity is increased from GPE-0 to GPE-7.5 with POSS filling amount. Then the ionic conductivity of GPE-10 decreases as POSS content further increases. The ionic conductivity of GPE-7.5 is the maximum. For GPE membrane, usually the liquid electrolyte uptake is one of the most important keys to improve ionic conductivity. The reason is that the more amount plasticizer endows the charge carriers of lithium ions in GPE with the easier movement ability. For GPE-10, although the uptake of liquid electrolyte is the maximum, the POSS in GPE keeps the crystalline structure and is not a good influence factor for ionic conductivity, which is evidenced in the discussion of XRD analysis of GPEs.

It also can be seen from the inset of **Fig. 5** that the imaginary part of the impedance is almost linearly related to its real part and the imaginary part increases more quickly than the real part when the frequency becomes lower, which demonstrates the characteristic of an equivalent of a resistor and a capacitor in series, corresponding to the resistance of the polymer electrolyte and the double capacitance of the cell in this case.

3.2.3. The relationship between ionic conductivity and temperature

The relationship between temperature and ion conductivity is used to analyze the mechanism of ionic conduction in six kinds of GPE membrane in the temperature range from 30°C to 55°C, which are shown in **Fig.6**. From **(a)** to **(f)**, the electrolyte bulk resistance $R_b(\Omega)$ is continuously decreased with temperature, which means the ionic conductivity is correspondingly increased. In GPE system, ionic conductivity of all samples increases with the temperature rise. This well-known phenomenon results from faster ion movement when the temperature increases and as a consequence leads to higher ionic conductivity. In addition, the motion of polymer chain is the movement driving force of current carriers of lithium ion, and the higher temperature endows the

polymer chain with more flexibility and enhances segmental mobility, which undoubtedly and ultimately is beneficial to improve the ionic conductivity. The ionic conductivity is reasonably determined by the Arrhenius equation,⁴⁷ which can be written as follows:

$$\sigma = A \exp(-E_a / \kappa T) \quad (4)$$

Where σ is the ionic conductivity; A is the pre-exponential factor; E_a is the activation energy; κ is the Boltzmann constant and T is the absolute temperature.

The dependence of ionic conductivity on temperature is shown in **Fig.7**. From (a) to (f), the corresponding linear relationship between $\lg\sigma$ and $1/T$ is the typical Arrhenius behavior.

Considering the ionic conductivity and self-standing property, GPE-7.5 was chosen to carry out the further investigation.

3.2.4 XRD analysis

XRD patterns of GPE membranes with different POSS/PMMA ratio are shown in **Fig.8**. The XRD spectrum of lithium salt indicates LiClO_4 is crystalline, but in the XRD curves of all GPEs there is not any obvious peaks of LiClO_4 more, which means LiClO_4 is completely dissociated. The kind of dissociation reaction produces the charge carriers of lithium ions in GPE. The pure PMMA XRD curve shows two obvious peaks, which hints that the purchased PMMA is a kind of crystalline polymer and must be synthesized by isotactic polymerization. From GPE-1 to GPE-7.5, there are very weak peaks of POSS in XRD patterns, indicates that the crystalline of POSS almost was destroyed. Whereas there are obvious peaks in GPE-10 XRD pattern, means POSS existed in crystalline. Combined with the above investigation of liquid electrolyte uptakes and ionic conductivity of GPEs with different POSS addition amount, it can be concluded that whether the POSS is crystalline or not, its modification action for GPE is remained, for example with POSS amount increasing the liquid electrolyte uptake is enhanced. But when POSS addition amount is high up to 10wt.%, the existed crystalline is not favorable to the movement of lithium ions and decreases the conductivity. In addition, compared to GPE-1 and GPE-2.5, GPE-5 shows a little more crystalline structure and higher ionic conductivity. This can be explained as that when POSS addition content is low, the ionic conductivity is mainly determined by the liquid electrolyte uptake, and the uptake value of GPE-5 is the highest in these three GPE systems.

3.2.5 Transference number

The lithium ion transference number, t_{Li^+} , is an important parameter for lithium ion batteries. The t_{Li^+} of GPE-7.5 is calculated with the value of 0.33, which is much higher than or near to that of many commercial separator and GPEs reported in references.⁴⁸⁻⁴⁹

3.2.6 Electrochemical stability

As a prerequisite and important step to characterize electrochemical performance of GPE, its electrochemical stability is elucidated by cyclic voltammogram (CV) in **Fig.10**. A pair of cathodic and anodic peaks appeared at around 0V, corresponding to the lithium redox processes:⁵⁰ on scanning the electrode in a negative direction, a cathodic peak is observed at about -0.35V, which corresponds to the plating of lithium onto the stainless steel electrode; on the reverse scanning, the stripping of lithium is observed at about 0.30V. In addition, the voltammograms ascribed to lithium deposition/dissolution is highly reversible, because the peak currents remain fairly considerable symmetry.⁵¹ The kind of highly reversible is favorable to the application of GPE in lithium ion batteries.

3.2.7 Electrochemical stability window

For practical battery applications, the electrochemical stability of electrolyte within the operation voltage of the battery system is very important. Linear sweep voltammogram (LSV) has been used in this study to investigate the electrochemical stability window (ESW).⁵² The electrochemical stability of GPE is evaluated by LSV measurement, as shown in **Fig. 11**. The current flow appears one flat when the voltage is below 5.25 V (vs. Li/Li⁺). The current onset at 5.25 V in the anodic voltage range results from a decomposition process associated with the electrolyte and such an onset voltage is considered as the upper limit of the electrolyte stability range, which can be assigned to the electrochemical decomposition voltages of GPE-7.5 and is a key application index in lithium ion batteries with high working voltage. So GPE-7.5 has electrochemical stability suitable to allowing the use of high-voltage electrode materials.

3.2.8 Compatibility with anode

The compatibility of GPE with lithium anode is very important for the safety and cycle performance when electrolyte is considered for application in lithium ion batteries, which can be evaluated on the interfacial resistance between lithium metal electrode and GPE.⁵³ The interfacial resistance is related to the passive layer and the charge transfer resistances on the lithium metal electrode.^{38,54} The EIS plots of the Li/GPE-7.5/Li symmetric cell for different storage time are demonstrated in **Fig.12**, which can clearly and directly reflect the compatibility between GPE and lithium anode.^{23,55} Combined with the amplified figure, all plots include two semicircles. The first high-frequency one is associated with ion transport resistance (R_p) in the passive layer formed on the lithium electrode surface through the chemical reaction between lithium and PC. The second semicircle at low frequencies which is associated with charge transfer resistance (R_{ct}) of the $\text{Li}^+ + \text{e}^- \leftrightarrow \text{Li}$ reaction. The summation of the two kinds of resistance is the interfacial resistance (R_i) of the electrode/electrolyte. For all EIS plots, there are two parts of semicircle. From the whole change trend, the interfacial resistance of the symmetrical cell Li/GPE-7.5/Li from **Fig.12** decreases from the first day to the 28 days. However it is known that R_p must increase because the thickness and structure of the formed passive layer change with storage time. So here it can be concluded that R_{ct} decreases with larger magnitude. The tremendous decrease of R_{ct} within 28 days is due to the activation of lithium electrode surface through the iterative process of $\text{Li}^+ + \text{e}^- \leftrightarrow \text{Li}$ reaction during the electrochemical impedance test. So GPE-7.5 shows wonderful compatibility with lithium anode.

4. Conclusion

The suitability of the membrane of POSS composited PMMA as host matrix for GPE used in lithium ion batteries is explored. The POSS addition amount is very key influence factor for performances of GPE. These performances of ionic conductivity, thermal stability, lithium ion transference number, electrochemical stability window and compatibility with lithium metal electrode of GPE7.5 obviously indicates that it can be used in lithium ion batteries as one kind of potential electrolyte candidate.

Acknowledgements

The authors gratefully acknowledge the financial support from the Specialized Research Fund for the Doctoral Program of Higher Education of China (20115121120005), Open Fund for the Oil and Gas Materials Key Laboratory of Higher Education of Sichuan Province (x151514kc104) and the Innovative Research Team of Sichuan Provincial Education Department.

References

- 1 P. Simon and Y. Gogotsi, *Nat. Mater.*, 2008, 7, 845.
- 2 J. M. Tarascon and M. Armand, *Nature*, 2001, 414, 359.
- 3 M. Armand and J. M. Tarascon, *Nature*, 2008, 451, 652.
- 4 X. Zuo, X. M. Liu, F. Cai, H. Yang, X. D. Shen and G. Liu, *J. Mater. Chem.*, 2012, 22, 22265.
- 5 J. M. Tarascon and M. Armand, *Nature*, 2001, 414, 359.
- 6 F. X. Wang, S. Y. Xiao, Y. Shi, L. L. Liu, Y. S. Zhu, Y. P. Wu and R. Holze, *Electrochim. Acta*, 2013, 93, 301.
- 7 Q. Lu, J. Fang, J. Yang, R. Miao, J. Wang and Y. Nuli. *J. Membr. Sci.*, 2014, 449, 176.
- 8 P.X. Yang, L. Liu, L.B. Li, J. Hou, Y.P. Xu, X. Ren, M.Z. An and N. Li. *Electrochim. Acta*, 2014, 115, 454.
- 9 K. Murata, S. Izuchi and Y. Yoshihisa, *Electrochim. Acta.*, 2000, 45, 1501.
- 10 D. He, D.W. Kim, J.S. Park, S.Y. Cho and Y. Kang, *J. Power Sources*, 2013, 244, 170.
- 11 K. Minami, A. Hayashi, S. Ujiie and M. Tatsumisago, *Solid State Ionic.*, 2011, 192, 122.
- 12 A.I.B. Rondão, S.G. Patrício, F.M.L. Figueiredo and F.M.B. Marques, *Electrochim. Acta*, 2013, 109, 701.
- 13 C.C. Cook and M.J. Wagner, *Electrochim. Acta*, 2013, 89, 778.
- 14 S.S. Sekhon, D.P. Kaur, J.S. Park and K. Yamada, *Electrochim. Acta*, 2012, 60, 366.
- 15 S. Oh, D.W. Kim, C. Lee, M. Lee and Y. Kang, *Electrochim. Acta*, 2011, 57, 46.
- 16 P. Isken, M. Winter, S. Passerini and A. Lex-Balducci. *J. Power Sources*, 2013, 225, 157.
- 17 J.M. Tarascon, A.S. Gozdz, C. Schmutz, F. Shokoohi and P.C. Warren, *Solid State Ionics*, 1996, 86-88, 49.
- 18 N.H. Idris, M.M. Rahman, J.Z. Wang and H.K. Liu, *J. Power Sources*, 202, 201, 294.
- 19 Y.F. Zhou, S. Xie and C.H. Chen, *J. Mater. Sci.*, 2006, 41, 7492.
- 20 M. Deka and A. Kumar, *Electrochim. Acta*, 2010, 55, 1836.

- 21 H. Akashi, M. Shibuya, K. Orui, G. Shibamoto and K. Sekai, *J. Power Sources*, 2002, 112, 577.
- 22 S.S. Zhang, K. Xu and T.R. Jow, *Solid State Ionics*, 2003, 158, 375.
- 23 M.M. Rao, J.S. Liu, W.S. Li, Y. Liang and D.Y. Zhou, *J. Membr. Sci.* 2008, 322, 314.
- 24 Y. Zhu, F. Wang and Y. Wu, *Energy Environ. Sci.*, 2013, 6, 618.
- 25 J. Cao, B. Zhu and Y. Xu, *J. Membr. Sci.*, 2006, 281, 446.
- 26 Y. Ding, P. Zhang and W. Di, *J. Membr. Sci.*, 2009, 329, 56.
- 27 H.S. Jeong, S.C. Hong and S.Y. Lee, *J. Membr. Sci.*, 2010, 364, 177.
- 28 K. Edelmann and B. Sandner, *Polym.*, 2005, 46, 397.
- 29 D. Kumar and S.A. Hashmi, *J. Power Sources*, 2010, 195, 5101.
- 30 J. Sharma and S. Sekhon, *Solid State Ionics*, 2007, 178, 439.
- 31 Y. Lee, S.H. Ju, J. Kim, S.S. Hwang, J. Choi, Y. Sun, H. Kim, B. Scrosati and D. Kim, *Electrochem. Commun.*, 2012, 17, 18.
- 32 H. Jeong, E. Choi, S. Lee and J.H. Kim, *J. Membr. Sci.*, 2012, 415-416, 513.
- 33 A. Chandra, A. Chandra and K. Thakur, *Composites Part B: Eng.*, 2014, 60, 292.
- 34 Y.H. Liao, M.M. Rao, W.S. Li, L.T. Yang, B.K. Zhu, R. Xu and C.H. Fu, *J. Membr. Sci.*, 2010, 352, 95.
- 35 T. Itoh, M. Yoshikawa, T. Uno and M. Kubo, *Ionics*, 2009, 15, 27.
- 36 Y. Liao, C. Sun, S. Hu and W. Li, *Electrochim. Acta*, 2013, 89, 461.
- 37 A. Chandra, A. Chandra and K. Thakur, *Composites: Part B*, 2014, 60, 292.
- 38 H. Xie, Y. Liao, P. Sun, T. Chen, M. Rao and W. Li, *Electrochim. Acta*, 2014, 2014, 127, 327.
- 39 M.E. Mackay, A. Tuteja, P.M. Duxbury, C. J. Hawker, B. Van Horn, Z. Guan, G. Chen and R.S. Krishnan, *Sci.*, 2006, 311, 1740.
- 40 Z. Zhou, L. Cui, Y. Zhang, Y. Zhang and N. Yin, *Eur. Polym. J.*, 2008, 44, 3057.
- 41 T. Nezakati, A. Tan and A.M. Seifalian, *J. Colloid Interf. Sci.*, 2014, 435, 145.
- 42 Y.Z. Liu, Y. Sun, F.L. Zeng, Q.H. Zhang and L. Geng, *Appl. Surf. Sci.*, 2014, 320, 908.
- 43 P.G. Bruce and C.A. Vincent, *J. Electroanal. Chem. Interfacial Electrochem.*, 1987, 225, 1.
- 44 M. Hoyos, A. Fina, F. Carniato, M. Prato and O. Monticelli, *Polym. Degrad. Stabil.*, 2011, 96, 1793.
- 45 A.B.V.K. Kumar, T.D. Thangadurai and Y.I. Lee, *React. Funct. Polym.*, 2013, 73, 1175.

- 46 W.Y. Nie, G. Li, Y. Li and H.Y. Xu, *Chinese Chem. Lett.*, 2009, 20, 738.
- 47 X. Ma, X. Huang, J. Gao, S. Zhang, Z. Deng and J. Suo, *Electrochim. Acta*, 2014, 115, 216.
- 48 S. Xiao, F. Wang, Y. Yang, Z. Chang and Y. Wu, *RSC Adv.*, 2014, 4, 76.
- 49 S. Zugmann, M. Fleischmann, M. Amereller, R.M. Gschwind, H.D. Wiemhöfer and H.J. Gores, *Electrochim. Acta*, 2011, 56, 3926.
- 50 D.W. Kim, Y.R. Kim, J.k. Park and S.I. Moon, *Solid State Ionics*, 1998, 106, 329.
- 51 I. Stepniak, *J. Power Sources*, 2014, 247, 112.
- 52 Y. Liao, M. Rao, W. Li, C. Tan, J. Yi and L. Chen, *Electrochim. Acta*, 2009, 54, 6396.
- 53 K.S. Kum, M.K. Song, Y.T. Kim, H.S. Kim, B.W. Cho and H.W. Rhee, *Electrochim. Acta*, 2004, 50, 285.
- 54 Y. Aihara, S. Arai and K. Hayamizu, *Electrochim. Acta*, 2000, 45, 1321.
- 55 Y.H. Liao, X.P. Li, C.H. Fu, R. Xu, M.M. Rao, L. Zhou, S.J. Hu and W.S. Li, *J. Power Sources*, 2011, 196, 6723.

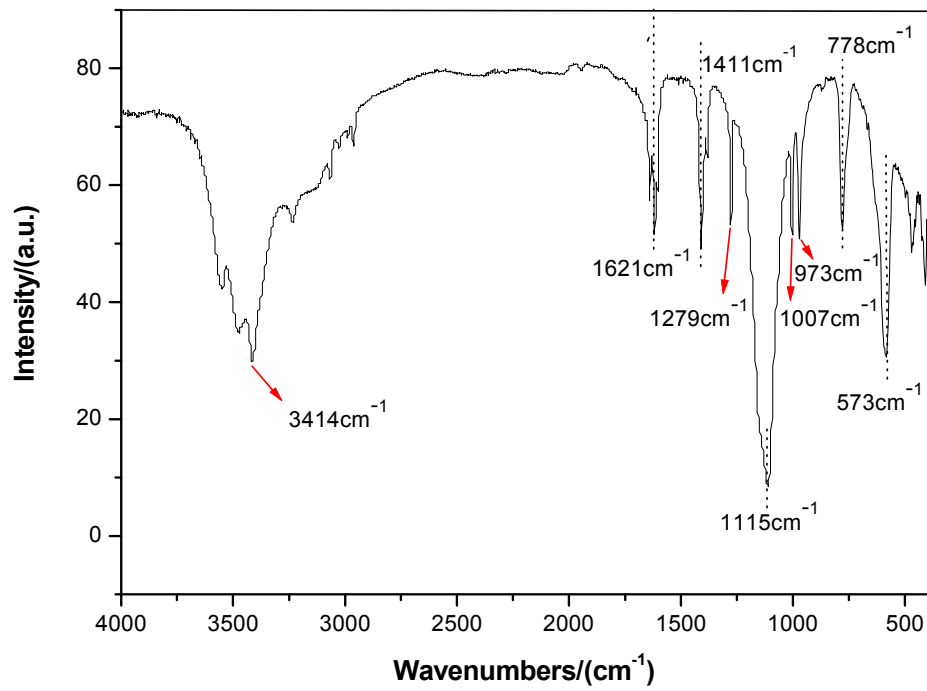


Fig.1 FTIR spectrum of POSS.

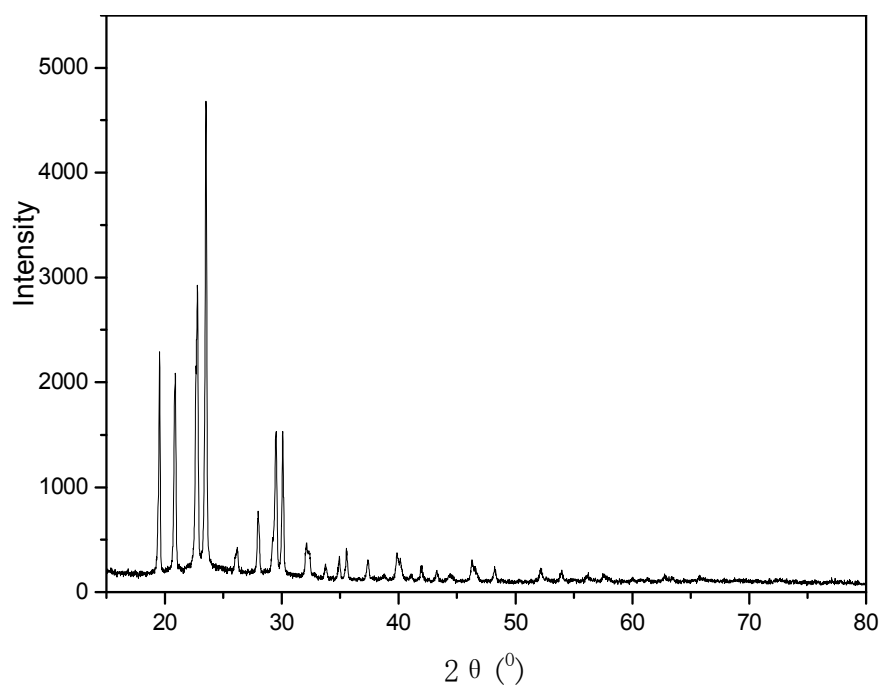


Fig.2 The XRD spectrum of POSS.

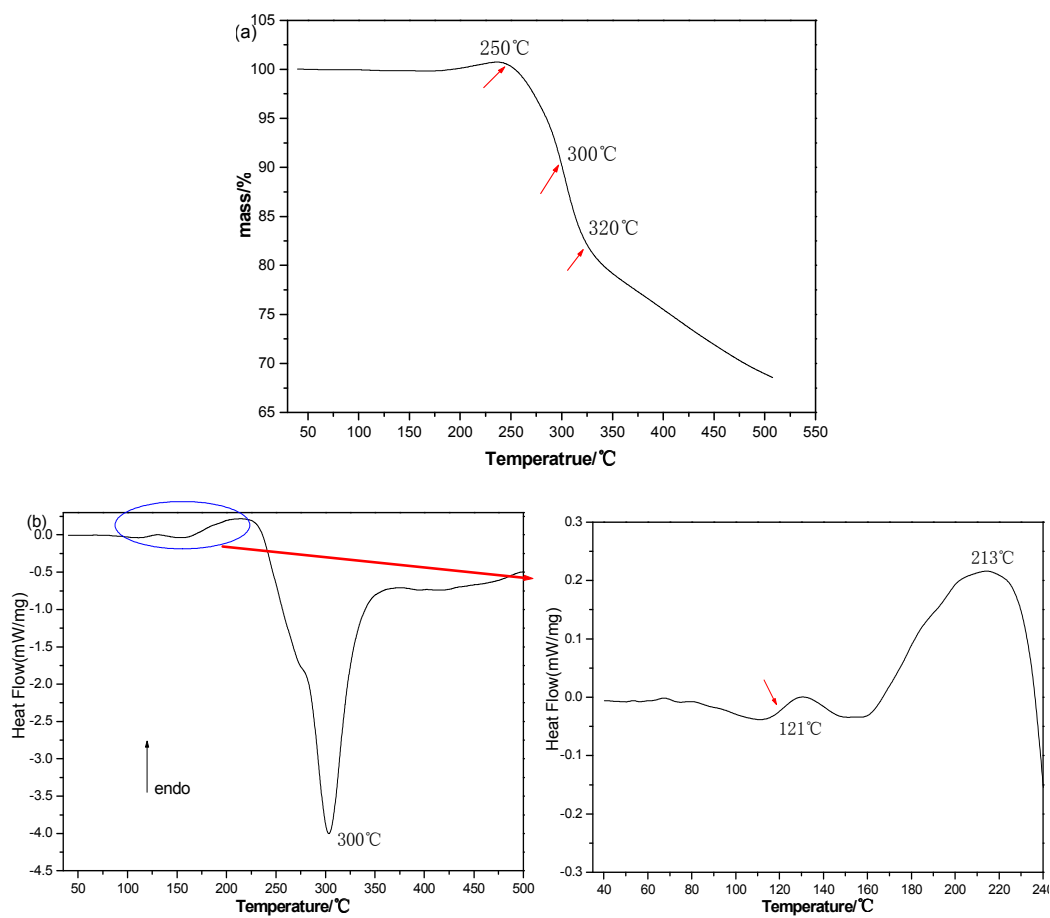


Fig.3 The (a) TGA and (b) DSC curves of POSS.

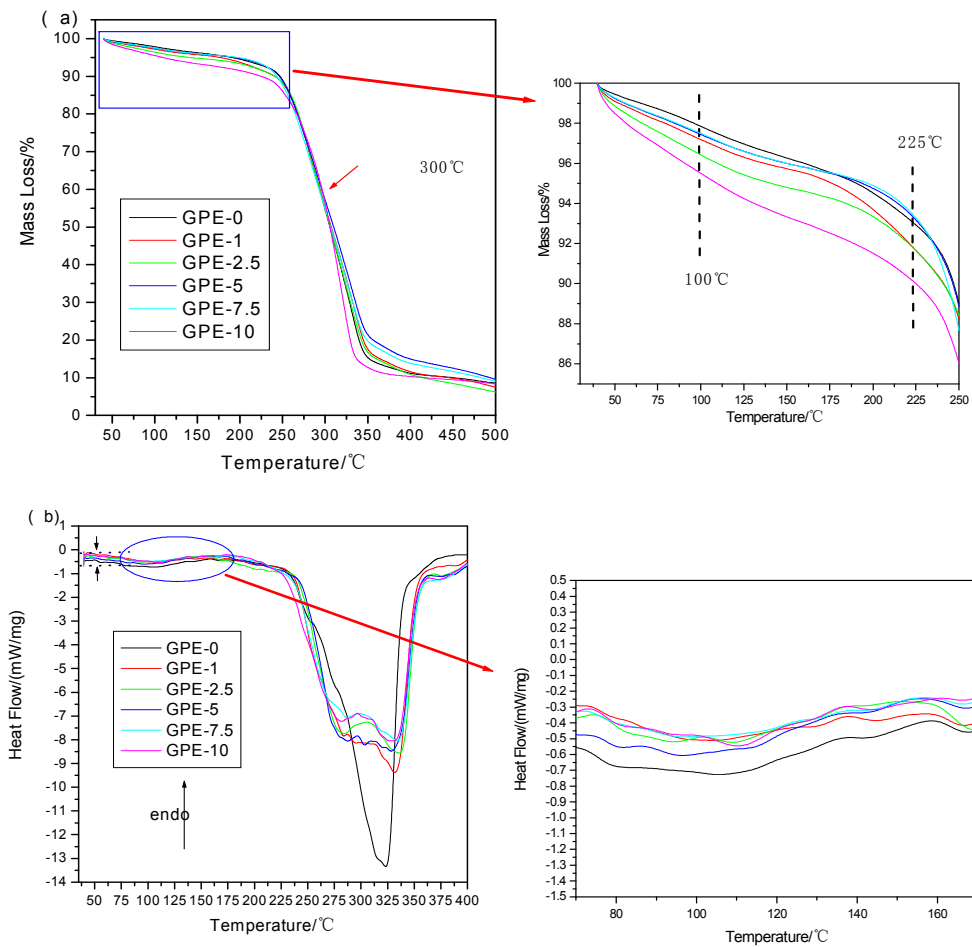


Fig.4 The (a) TGA and (b) DSC curves of GPEs.

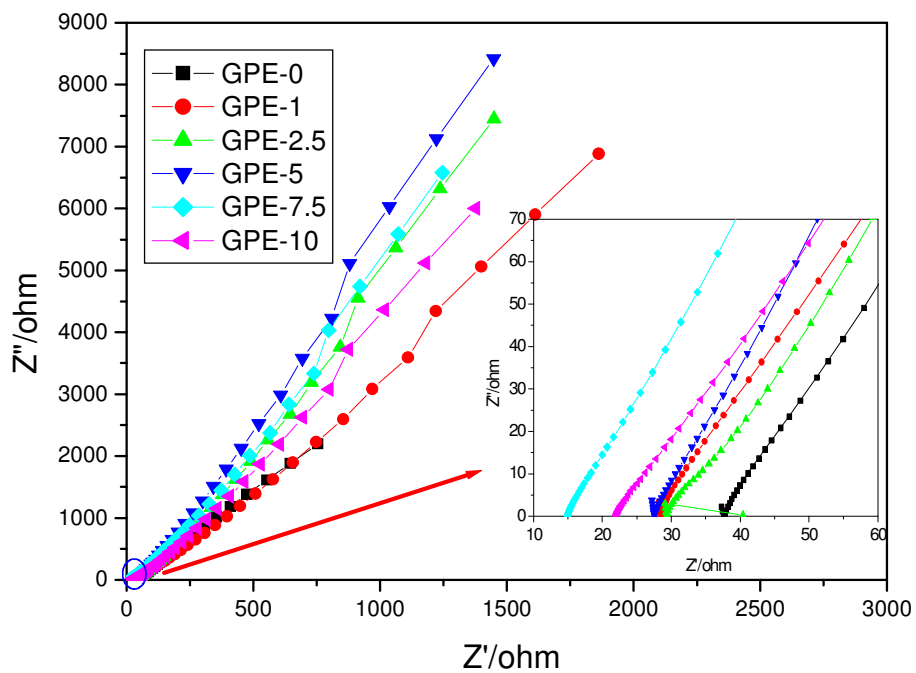


Fig.5 The EIS spectra of GPEs.

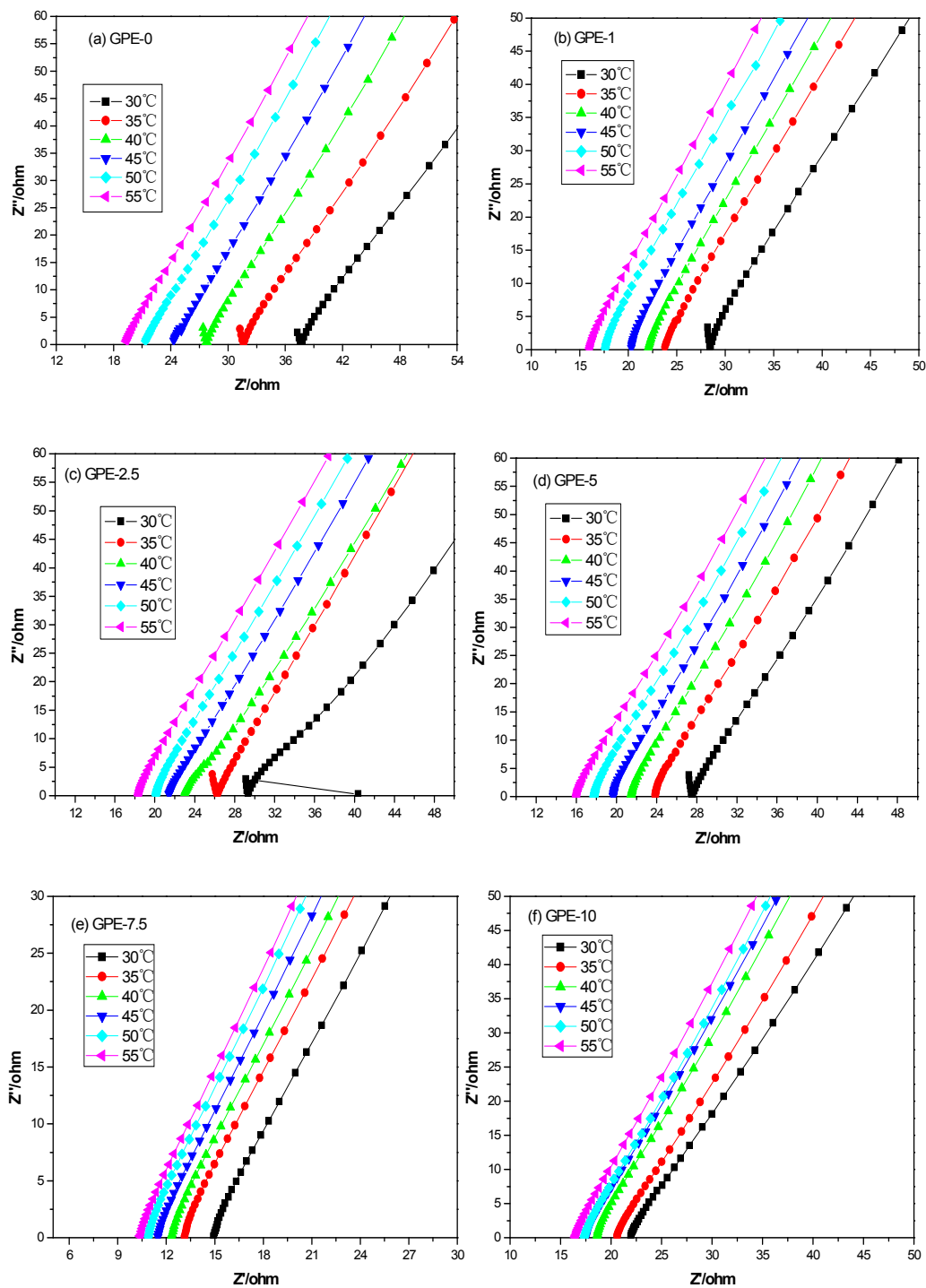


Fig.6 The EIS of (a)GPE-0, (b)GPE-1, (c)GPE-2.5, (d)GPE-5, (e)GPE-7.5 and (f)GPE-7.5 at different temperature.

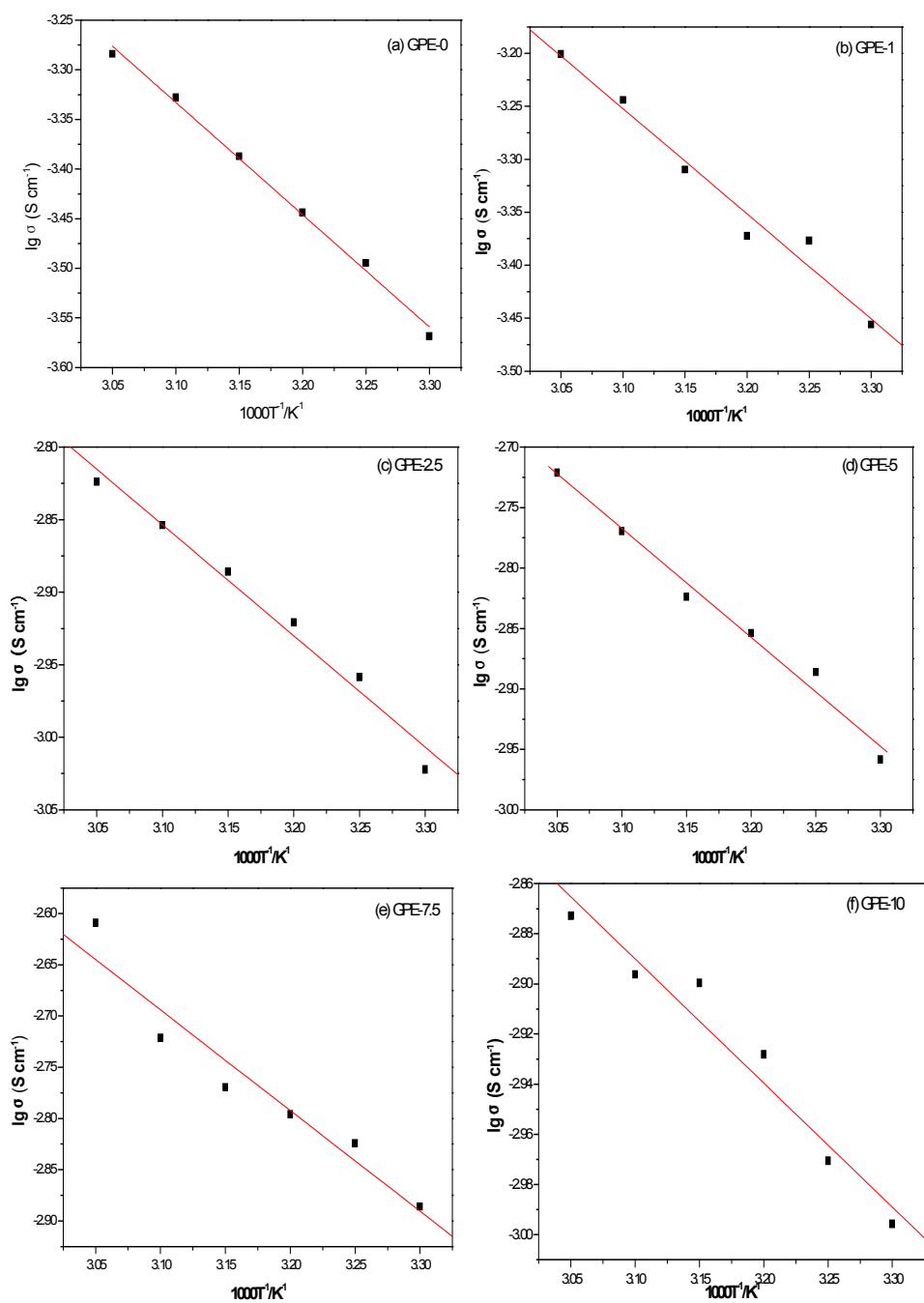


Fig.7 The dependence of ionic conductivity of (a)GPE-0, (b)GPE-1, (c)GPE-2.5, (d)GPE-5, (e)GPE-7.5 and (f)GPE-10 on temperature.

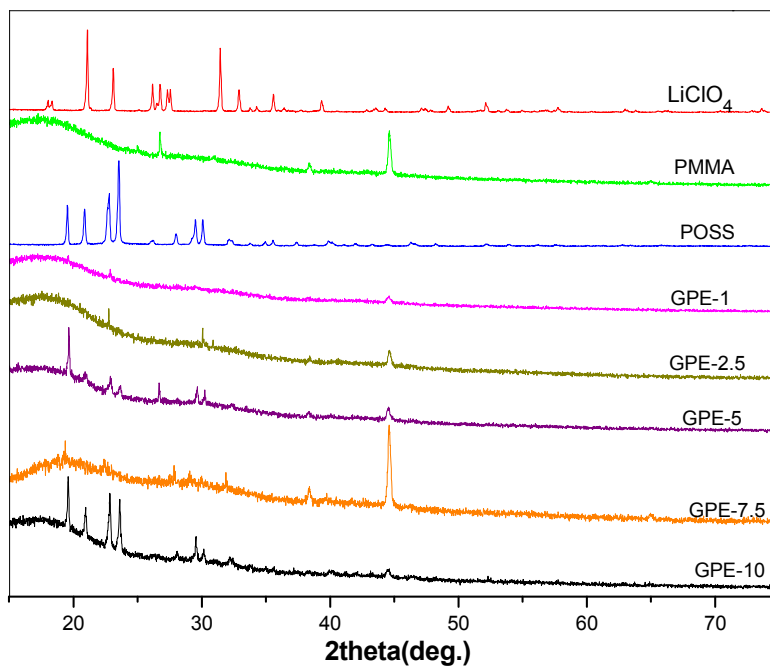


Fig.8 The XRD spectra of LiClO₄, PMMA, POSS, GPE-1, GPE-2.5, GPE-5, GPE-7.5 and GPE-

10.

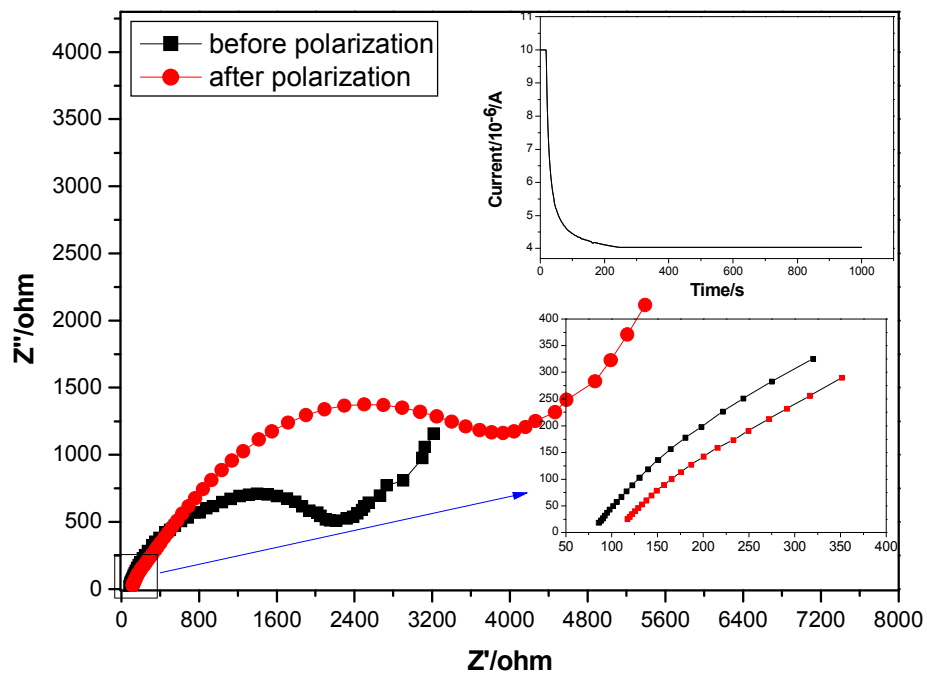


Fig.9 Impedance spectra of the Li/GPE/Li cell measured before and after polarization.

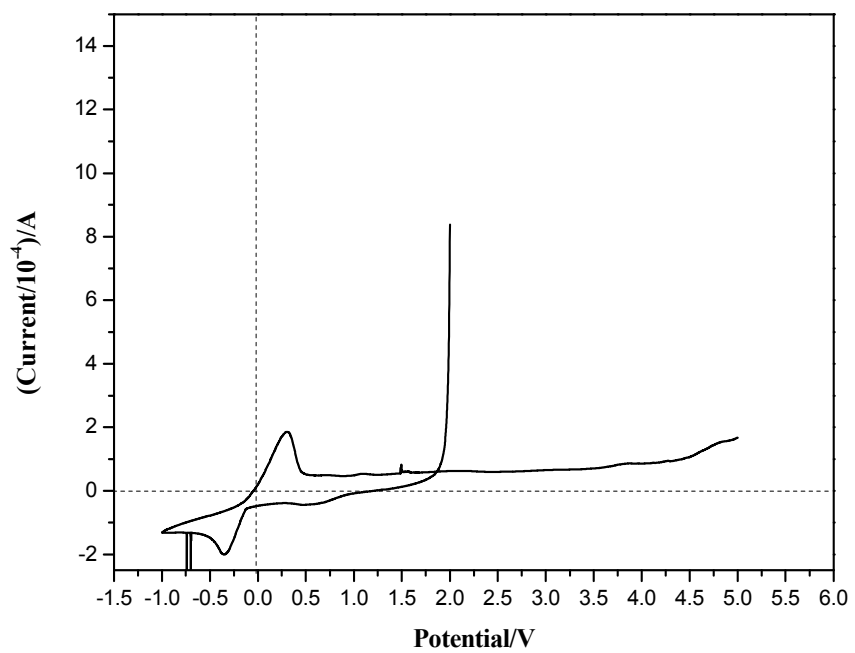


Fig.10 The cyclic voltammogram of Li/GPE/SS cell.

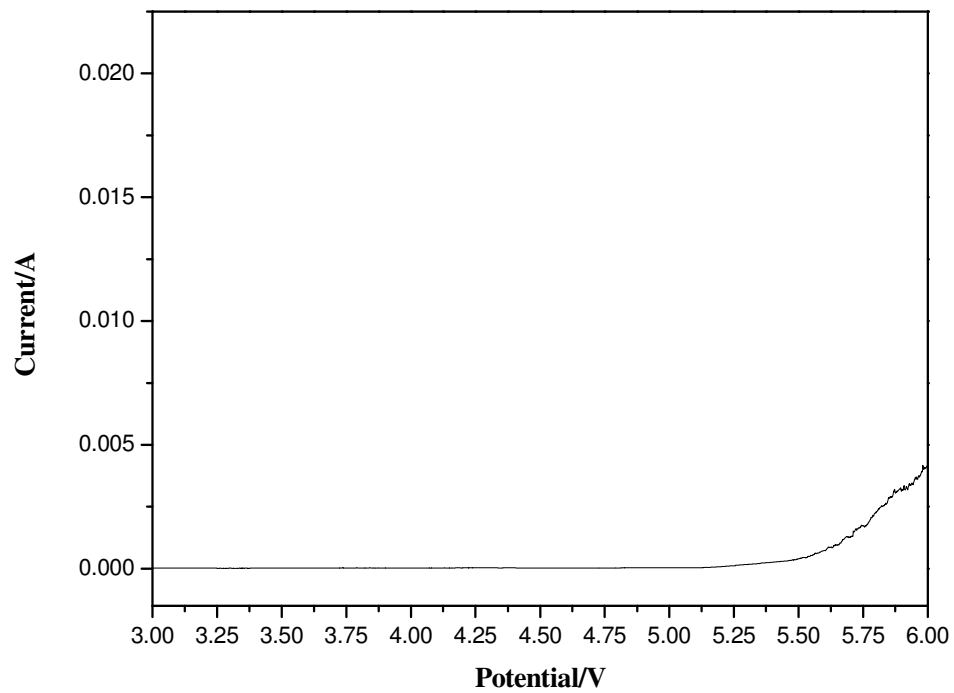


Fig.11 Linear sweep voltammogram of Li/GPE/SS cell.

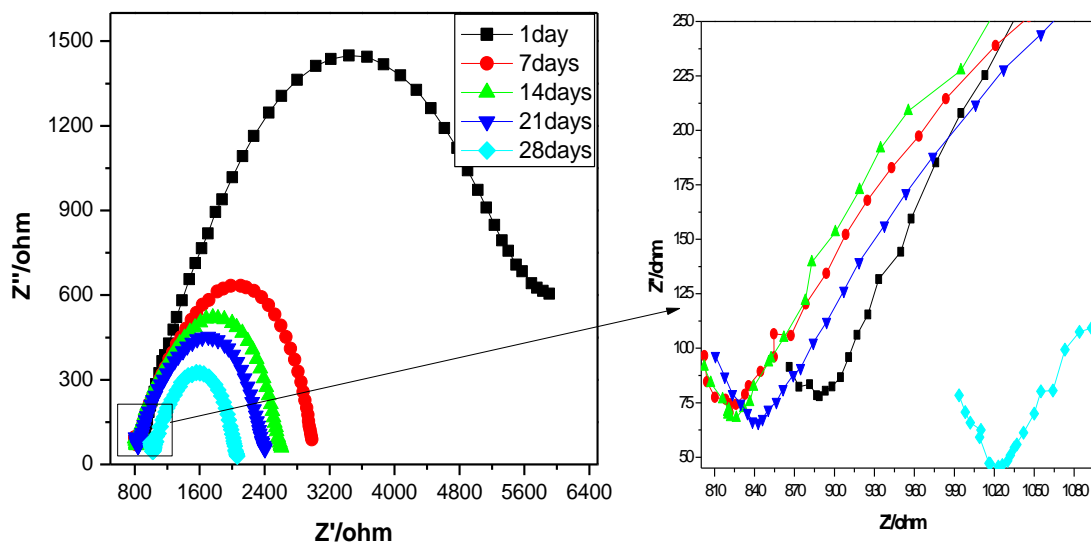


Fig.12 Electrochemical impedance spectra of Li/GPE/Li cell.

Table.1 The GPEs with different POSS content.

GPE	GPE-0	GPE-1	GPE-2.5	GPE-5	GPE-7.5	GPE-10
POSS/ g	0.000	0.010	0.025	0.050	0.075	0.100
PMMA/ g	1.000	0.990	0.975	0.950	0.925	0.900

Table.2 The uptake value and ionic conductivity of GPEs.

Samples	Uptake <i>A</i> (wt.%)	Ionic conductivity($\times 10^{-4}$ S cm $^{-1}$)
GPE-0	61	2.7
GPE-1	100	3.5
GPE-2.5	104	9.5
GPE-5	108	10.9
GPE-7.5	120	13.3
GPE-10	126	10.1